Hexahydro-1,2,3-triazine Derivatives: Synthesis, Antimicrobial Evaluation, Antibiofilm Activity and Study of Molecular Docking Against Glucosamine-6-Phosphate

Nabel Bunyan Ayrim[1*], Fadhel Rukhis Hafedh[1], Yasir Mohamed Kadhim[2], Abduljabbar Sabah Hussein[1], Ahmed Mutanabbi Abdula[1], Ghosoun Lafta Mohsen[3], and Mohammed Mahdi Sami[4]

[1]*Department of Chemistry, College of Science, Mustansiriyah University, Baghdad 10052, Iraq*

[2]*Department of Pharmaceutical Chemistry, College of Pharmacy, Al-Nahrain University, Baghdad 10072, Iraq*

[3]*Department of Chemistry, College of Science, Al- Nahrain University, Baghdad 10072, Iraq*

[4]*Department of Remote Sensing and Geophysics, College of Science, Alkarkh University, Baghdad 10011, Iraq*

Corresponding author:

email:
nabelbunyan@uomustansiriyah.edu.iq

Received: June 10, 2023
Accepted: September 15, 2023

DOI: 10.22146/ijc.85521

Abstract: *The* N,N',N''*-trisubstituted hexahydro-1,3,5-triazine derivatives (**3a**–**g**) had been created and identified through infrared, nuclear magnetic resonance, and mass spectrometry according to their symmetric basic structure. Three molecules of diverse aromatic amines and three molecules of formaldehyde were assembled in a "1+1+1+1+1+1" condensation reaction to produce hexahydrotriazines. Two Gram-positive (*Staphylococcus aureus, Staphylococcus epidermidis*) and two Gram-negative (*Klebsiella pneumonia, Pseudomonas aeruginosa*) bacteria were used to evaluate the antimicrobial activity of the produced compounds. The anti-biofilm activity of **3g** against* S. aureus *was also examined. In this investigation, glucosamine-6-phosphate synthase was employed to investigate the binding affinity of **3g** within the enzyme's binding site. The results demonstrated that most of the synthesized hexahydro-1,3,5-triazine compounds have mild antimicrobial effects in comparison with the commonly used drug ampicillin, whereas the compounds **3g** are potentially anti-biofilm agents. Molecular docking with the Autodock 4.2 tool was applied to study the binding affinity. It was found to hit (**3g**) in the active center of glucosamine-6-phosphate synthase as the target enzyme for antimicrobial agents.* In silico *studies reveal that the discovered hit is a promising glucosamine-6-phosphate inhibitor, as well as that the docking data matched up to the* in vitro *assay.*

Keywords: *1,3,5-hexahydrotriazines; antimicrobial; antibiofilm; docking study*

■ INTRODUCTION

A biofilm is a complicated accumulation process of every species of organism, including bacteria, fungi, yeasts, algae, protozoa, and viruses, that is fixed to surfaces, spreads wildly and promptly, and is difficult to eliminate completely. This is due to the fact that their preferred method of growth is built in a matrix that consists of exopolysaccharides and released nucleic acids, which preserve it from outside influences such as antibiotics and biocides [1]. Diseases include cystic fibrosis-related pneumonia, as well as endocarditis, periodontitis, endocarditis, osteomyelitis, and urinary tract infections, are all caused by biofilms [2]. Moreover, they have been linked to the inhibition of wound recuperation in chronic lesions [3]. The prevalence of antibiotic resistance among biofilm-associated microorganisms is extremely high. These resistant features and the genetic and morphological diversity of biofilm cells inspired researchers to begin looking for new antibacterial agents with novel mechanisms of action [4]. Heterocyclic scaffolds containing nitrogen are common in medicinal drugs, synthetic bioactive compounds, and natural chemicals like alkaloids [5]. Therefore, the scientific study organization decided to concentrate on this component by synthesizing new 1,3,5-hexahydrotriazines, which have three atoms of nitrogen at 1, 3, and 5 sites and are

six-membered ring structures [6].

It has been demonstrated that heterocyclic compounds exhibit a diverse range of biological and pharmacological actions. In particular, these activities include antimalarial [7], antitumor, antimicrobial [8], antibacterial [9], anticancer [10], anti-HSV-1, antifungal [11], anticorrosive [12], anti-HIV [13], antimethamphetamine action, treatment of Alzheimer's disease, anti-angiogenic activity, anti-trypanosomal drugs, anti-viral drugs, treatment of autoimmune disease [14], and showing potent antidiabetic activity [15]. The field of industrial chemistry is becoming increasingly interested in a wide variety of triazine derivatives, particularly for their potential use as inhibitors of corrosion in the oil and gas industry [16]. The 1,3,5-triazines form the backbones of a number of herbicides, fungicides, and insecticides, e.g., anilazine (fungicide), menazon (insecticide), simazine, atrazine, cyanazine, and prometon (herbicides) [17].

Glucosamine-6-phosphate synthase (GlcN-6-PS) is recognized as a suitable target for the docking study against antimicrobial agents, as illustrated in previous studies. GlcN-6-PS is an essential enzyme for the formation of *N*-acetyl glucosamine, the fundamental component of bacterial and fungal cell walls [18-20]. The major objective of the work was to develop a synthetic series of 1,3,5-triazinane (**3a**-**g**) and describe them using spectral data. The 1,3,5-triazinane derivatives were tested in the laboratory with a variety of bacterial species (Gram-positive and Gram-negative) and found to have moderate to potent effects. The compound **3g** was tested for antibiofilm inhibitory action against *S. aureus* in an LB growth medium using an Elisa reader. The results demonstrate that compound **3g** has three times the ability to limit biofilm formation. We have explored the connecting affinities for hit **3g** within the enzyme's activation pocket. The docking results were in agreement with the *in vitro* antimicrobial assay.

■ EXPERIMENTAL SECTION

Materials

All used compounds were 37% aqueous formaldehyde, *p*-methylaniline, *p*-ethoxyaniline, *p*-chloroaniline, *p*-bromoaniline, *p*-aminobenzoic acid, *p*-nitroaniline, and *p*-methoxyaniline from Sigma Aldrich. Ethanol and petroleum ether were purchased from Alpha Chemika with a purity of between 95 and 98% with no further purification.

Instrumentation

A Gallen-Kamp MFB-600 melting point apparatus was utilized to measure the melting points for all crystalline materials in open capillary tubes without any corrections. Thin-layer chromatography (TLC) with eluents of *n*-hexane:ethyl acetate was used to observe the TLC spots that formed during the reactions in this work. Using an FTIR 8400S-Shimadzu spectrophotometer (Japan), IR spectra with a range of 400–4000 cm^{-1} were used to characterize the synthesized compounds. A Shimadzu model GCMSQP 1000 EX spectrometer from Japan was used to record mass spectra. The ^{1}H- and ^{13}C-NMR spectra were obtained with a VARIAN-INOVA 500 MHz spectrophotometer (Germany) with $CDCl_3$ and DMSO-d_6 as solvents, and tetramethylsilane TMS as an internal standard. The tests of the ^{1}H- and ^{13}C-NMR spectra were carried out at the Higher School of Chemistry/Sharif University, Tehran University, Iran.

Procedure

Synthesis of 1,3,5-hexahydrotriazine derivatives (3a-g)

A 100 mL round-bottomed flask was used to dissolve *p*-substituted aniline (**1a**-**g**, 5 mmol) in ethanol (30 mL). Then, 37% aqueous formaldehyde (2, 0.6 mL, 15 mmol) was subsequently added, and the mixture was shaken constantly for 24 h at room temperature. The crude product was filtered off when the reaction had finished, as determined by TLC, and washed with cold ethanol. To obtain the compounds **3a**-**g**, the products were further purified by recrystallization with boiled petroleum ether [21].

1,3,5-tri-*p*-tolyl-[1,3,5]triazinane (3a). White powder, yield: 78%; M.P: 186–190 °C; M.F: $C_{24}H_{27}N_3$; M.W: 357.50 g/mol; IR (cm^{-1}): 3020–3001 (C–H, aromatic), 2968–2858 (C–H, aliphatic), 1570 (C=C, aromatic), 1464 (CH_2, bending) 1373 (CH_3, bending). ^{1}H-NMR (500 MHz, $CDCl_3$, δ ppm): 2.28 (s, 9H, 3 *p*-

CH_3), 4.79 (s, 6H, C2H, C4H, C6H, CH_2-N, triazinane), 6.96 (d, J = 8.2 Hz, 6H, C2H, C6H, aromatic), 7.06 (d, J = 8.3 Hz, 6H, C3H, C5H, aromatic). ^{13}C-NMR (126 MHz, $CDCl_3$, δ ppm): 146.36 (3C, C1, -N-*ph*), 130.38 (3C, C4, aromatic), 129.71 (6C, C3, C5, aromatic), 118.01 (6C, C2, C6 aromatic), 69.55 (3C, C2, C4, C6, CH_2-N, triazinane), 20.55 (3C, *p*-CH_3). MS-EI (*m/z*, %): 357 (M^+, 10), 238 (30), 119 (100), 91(25).

1,3,5-Tris-(4-ethoxy-phenyl)-[1,3,5]triazinane (3b). White powder, yield: 71%; M.P: 83–85 °C; M.F: $C_{27}H_{33}N_3O_3$; M.W; 447.58 g/mol; IR (cm^{-1}): 3045 (C–H, aromatic), 2978–2825 (C–H, aliphatic), 1579 (C=C, aromatic), 1475 (CH_2, bending) 1392 (CH_3, bending), 1238 (C–O–C, ether). ^{1}H-NMR (500 MHz, $CDCl_3$, δ ppm): 1.42 (t, J = 7.2 Hz, 9H, 3 CH_3), 4.11 (q, J = 7.5 Hz, 6H, 3 OCH_2), 5.43 (s, 6H, C2H, C4H, and C6H, CH_2-N, triazinane), 6.75 (d, J = 8.0 Hz, 6H, C2H, and C6H, aromatic), 7.30 (d, J = 8.2 Hz, 6H, C3H and C5H, aromatic). ^{13}C-NMR (126 MHz, $CDCl_3$, δ ppm): 154.53 (3C, C4, -O-*ph*), 144.35 (3C, C1, -N-*ph*), 121.62 (6C, C3, C5, aromatic), 117.92 (6C, C2, C6, aromatic), 87.25 (3C, C2, C4, C6, CH_2-N, triazinane), 67.65 (3 OCH_2), 15.82 (3C, 3 CH_3). MS-EI (*m/z*, %): 447 (M^+, 8), 420 (5), 402 (9), 354 (10), 326 (100), 309 (50), 280 (19), 270 (50), 177 (25), 150 (15), 81 (30).

1,3,5-Tris(4-chlorophenyl)-1,3,5-triazinane (3c). White powder, yield: 74%; M.P: 241–245 °C; M.F: $C_{21}H_{18}Cl_3N_3$; M.W; 418.75 g/mol; IR (cm^{-1}): 3040–3000 (C–H, aromatic), 2939–2854 (C–H, aliphatic), 1595 (C=C, aromatic), 1494 (CH_2, bending), 808 (*para*-Cl). ^{1}H-NMR (500 MHz, DMSO-d_6, δ ppm): 4.93 (s, 6H, C2H, C4H, C6H, CH_2-N, triazinane), 7.08 (d, J = 8.4 Hz, 6H, C2H, C6H, aromatic), 7.20 (d, J = 8.4 Hz, 6H, C3H, C5H aromatic). ^{13}C NMR (126 MHz, DMSO-d_6, δ ppm): 147.53 (3C, C1, -N-*ph*), 129.08 (6C, C3, C5, aromatic), 124.18 (3C, C4-Cl), 119.09 (6C, C2, C6, aromatic), 67.30 (3C, C2, C4, C6, CH_2–N, triazinane). MS-EI (*m/z*, %): 417 (M^+, 100), 389 (16), 309 (55), 294 (35), 154 (40), 79 (40), 46 (18).

1,3,5-Tris(4-bromophenyl)-1,3,5-triazinane (3d). Gray powder, yield: 70%; M.P: 198–200 °C; M.F: $C_{21}H_{18}Br_3N_3$; M.W; 552.11 g/mol; IR (cm^{-1}): 3093–3076 (C–H, aromatic), 2928–2843 (C–H, aliphatic), 1587 (C=C, aromatic), 1489 (CH_2, bending), 806 (*para*-Br). ^{1}H-NMR (500 MHz, DMSO-d_6, δ ppm): 4.92 (s, 6H, C2H, C4H, C6H, CH_2–N, triazinane), 7.03 (d, J = 8.5 Hz, 6H, C2H, C6H, aromatic), 7.32 (d, J = 8.5 Hz, 6H, C3H, C5H aromatic). ^{13}C-NMR (126 MHz, DMSO-d_6, δ ppm): 147.86 (3C, C1, -N-*ph*), 131.97 (6C, C3, C5, aromatic), 119.46 (6C, C2, C6, aromatic), 111.96 (3C, C4-Br), 66.99 (3C, C2, C4, C6, CH_2-N, triazinane). MS-EI (*m/z*, %): 552 (M^+, 15), 479 (20), 464 (95), 434 (47), 386 (100), 384 (55), 330 (25), 321(20), 278 (36), 201 (24), 171 (20).

4,4′,4″-(1,3,5-Triazinane-1,3,5-triyl) tribenzoic acid (3e). White powder, yield: 71%; M.P: 210–214 °C; M.F: $C_{24}H_{21}N_3O_6$; M.W: 447.45 g/mol; IR (cm^{-1}): 3200–2400 (O–H), 3084–3003 (C–H, aromatic), 2947–2860 (C–H, aliphatic), 1666 (C=O), 1566 (C=C, aromatic), 1423 (CH_2, bending), 1329–1217 (C–O–C, ether). ^{1}H-NMR (500 MHZ, DMSO-d_6, δ ppm): 5.17 (s, 6H, C2H, C4H, C6H, CH_2–N, triazinane), 6.91 (d, J = 8.5 Hz, 6H, C2H, C6H, aromatic), 7.58 (d, J = 8.5 Hz, 6H, C3H, C5H, aromatic), 12.26 (s, 3H, COOH). ^{13}C-NMR (126 MHz, DMSO-d_6, δ ppm): 167.66 (3C, C=O), 148.73 (3C, C1, -N-*ph*), 130.54 (6C, C3, C5, aromatic), 120.94 (3C, C4–C=O), 113.92 (6C, C2, C6, aromatic), 82.25 (3C, C2, C4, C6, CH_2–N, triazinane). MS-EI (*m/z*, %): 447 (M^+, 16), 394 (20), 354 (14), 308 (34), 279 (14), 252 (100), 211 (34), 191 (40), 174 (20), 147 (88), 134 (48), 81 (75), 46 (18).

1,3,5-Tris(4-nitrophenyl)-1,3,5-triazinane(3f). Yellow powder, yield: 82%; M.P: 236–240 °C; MF: $C_{21}H_{18}N_6O_6$; MW: 450.41 g/mol; IR (cm^{-1}): 3080–3003 (C–H, aromatic), 2924–2825 (C–H, aliphatic), 1599 (C=C, aromatic), 1529–1319 (NO_2), 1469 (CH_2, bending).^{1}H-NMR (500 MHz, DMSO-d_6, ppm): 4.71 (s, 6H, C2H, C4H, C6H, CH_2-N, triazinane), 6.81 (d, J = 7.5 Hz, 6H, C2H, C6H, aromatic), 8.04 (d, J = 7.6 Hz, 6H, C3H, C5H aromatic). ^{13}C-NMR (126 MHz, DMSO-d_6, ppm): 153.71 (3C, C4-NO_2), 137.24 (3C, C1, -N-ph), 126.49 (6C, C3H, C5H, aromatic), 112.04 (6C, C2H, C6H, aromatic), 51.44 (3C, C2, C4, C6, CH_2–N, triazinane). MS-EI (*m/z*, %): 450 (M^+, 28), 412 (14), 350 (55), 279 (25), 256 (50), 240 (60), 218 (40), 151 (100), 138 (85), 81 (70), 46 (30).

1,3,5-tris(4-methoxyphenyl)-1,3,5-triazinane (3g). Gray powder, yield: 78%; M.P: 126–128 °C; M.F: $C_{24}H_{27}N_3O_3$; M.W; 405.50 g/mol; IR (cm^{-1}): 3090–3022

(C–H, aromatic), 2918–2854 (C–H, aliphatic), 1570 (C=C, aromatic), 1464 (CH_2, bending), 1325 (CH_3, bending), 1261 (C–O–C, ether). ^{1}H-NMR (500 MHz, DMSO-d_6, δ ppm): 3.67 (s, 9H, 3 *p*-OCH_3), 4.66 (s, 6H, C2H, C4H, C6H, CH_2-N, triazinane), 6.79 (d, J = 8.6 Hz, 6H, C3H, C5H, aromatic), 7.03 (d, J = 8.8 Hz, 6H, C2H, C6H, aromatic). ^{13}C-NMR (126 MHz, DMSO-d_6, δ ppm): 153.92 (3C, C4-OCH_3), 142.79 (3C, C1, -N-ph), 119.51 (6C, C3H, C5H, aromatic), 114.67 (6C, C2H, C6H aromatic), 69.87 (3C, C2, C4, C6, CH_2-N, triazinane), 55.63 (3C, *p*-OCH_3). MS-EI (*m/z*, %): 406 (M^+,10), 392 (100), 268 (100),149 (20),133 (14).

In vitro *antimicrobial activity*

The technique of disc diffusion was used to assess the antimicrobial effects of the compounds **3a**-**g**. Antibacterial activity was evaluated via *in vitro* culture against two Gram-positive (*S. aureus* and *S. epidermidis*) and two Gram-negative (*K. pneumonia, P. aeruginosa*) bacteria [22]. Bacterial strains were propagated by subculturing on nutrient agar in an incubator (37 °C) for 24 h. An amount of 20 mL of nutritional agar was sterilized and then placed in a Petri dish. The cultures of the bacterial strains were adjusted to grow at a McFarland value of 0.5 standards. Following the inoculation of the dishes with the bacterial strains, a period of 15 min was allowed for the adsorption of the strains into the gel. A sterile cork borer with a diameter of 6 mm was used to create wells in the gel. The test materials were dissolved in dimethyl sulfoxide (DMSO) at a volume of 200 µg/mL in each well. Ampicillin was used as the reference medication at a concentration of 200 µg/mL, and DMSO (1 µL) was used as a blank (solvent). After 24 h, the zones of inhibition were calculated [23-24].

Antibiofilm activity

Biofilm formation by *S. aureus* was evaluated in the presence of recently produced compounds. Overnight, bacteria were cultured in LB medium at 37 °C. Next, 100-fold dilutions were made in tryptone soybean broth (TSB) for *S. aureus* biofilm development. Each sample (200 µL) containing 5, 10, 20, 40, 50, 100, or 200 µM of compound **3g** was deposited in an SPL 96-well microplate. For 24 h, the plate was kept at 37 °C. An Elisa reader (BioTek Instruments, Inc., USA) set to 630 nm was used to assess cell proliferation. Using 10 mM phosphate-buffered saline solution (pH 7.4) for three times, the unattached cells were removed from the plate and dried at 50–60 °C for 1 h. After 15 min at the temperature of the room, a 0.1% (v/v) solution of crystal violet (CV) (200 µL) was poured into each well. After completely washing away the dye with standard water, the plate was allowed to dry for an additional hour at 50–60 °C. In order to extract the attached dye, 200 µL acetic acid 33% (v/v) was added at the final stage. An Elisa reader was then used to measure the absorbance at 570 nm. The DMSO concentration in every sample examined is the same, and a sample that just contains DMSO was also tested as a control [25].

Molecular docking

From the Protein Data Bank (PDB code 1MOQ), the crystal structure of GlcN-6-PS was selected and used as a rigid molecule. The native ligand and water molecules were removed from the enzyme in preparation for modelling. All docked compounds were created as mol files in Chem Draw Ultra 7.0., and using the software Open Babel 2.3.1, compound energies were reduced and then transformed to the pdb format. The grid size during docking was 60 × 60 × 60 Å with dots separated by 0.375 Å. The coordinates for X, Y, and Z have been specified as 31.0, 17.0, and −2.0, respectively. As the docking algorithm, the Lamarckian Genetic Algorithm was used, with a maximum number of 27,000 generations, 10 runs, 150 population sizes, and 2,500,000 energy evaluations [26-27].

■ RESULTS AND DISCUSSION

The 1,3,5-hexahydrotriazines become the target of much structural study because of their possible applications in the medical and chemical industries. The compounds are stable at ambient temperatures and yield suitable results. The symmetrically *N,N′,N″*-trisubstituted hexahydro-1,3,5-triazine derivatives **3a**-**g** were synthesized from the condensation reaction of various *p*-substituted anilines (4-methylaniline, 4-ethoxyaniline, 4-chloroaniline, 4-bromoaniline, 4-aminocarboxylic acid, 4-nitroaniline, 4-methoxyaniline,

and aqueous formaldehyde in ethanol [8]), outlined in Scheme 1. The structures of the target compounds **3a**-**g** were confirmed through the analysis of various spectroscopic techniques, including IR, ^{1}H-NMR, ^{13}C-NMR, and mass spectrometry. The ^{1}H-NMR spectra indicated the existence of singlet lines and two doublet signals at 5.43–4.66 and 8.0–4.75 ppm, which correspond to -CH_2-N of triazinane and aromatic protons, respectively. The IR spectra exhibited distinct bands of absorption between 1494–1423 cm^{-1} (CH_2, bending). The ^{13}C-NMR spectra indicated the existence of -CH_2-N, triazinane, between 87.25–51.4 ppm in addition to signals from each of the different atoms of carbon. Mass spectrum analysis showed [M^+] for all hexahydro-1,3,5-triazine derivatives**,** confirming their chemical formula. The details of the data are presented in the experiment part. Fig. 1 illustrates the mechanism of this condensation, which involves the reaction of nucleophilic species with formaldehyde to generate an imine, which then trimerizes to form 1,3,5-hexahydrotriazine [28].

In Vitro Antimicrobial Assays

Major structural differences between **3a**-**g** are only at the *para* location of the aniline part. The synthetic compounds were evaluated for antibacterial effects with Gram-positive (*S. aureus* and *S. epidermidis*) and Gram-negative (*K. pneumonia* and *P. aeruginosa*) bacteria. Compounds **3a**-**f** had moderate antibacterial activity against *S. aureus* with inhibition zone diameters ranging from 8 to 15 mm, while compound **3g** had greatest antibacterial effect, in a 21 mm diameter area of inhibition. Compounds **3a**-**g** demonstrated moderate antibacterial activity against *S. epidermidis*, with inhibition zone diameters ranging from 8 to 15 mm. Compounds **3a**-**g** had modest antibacterial activity against *P. aeruginosa* with inhibition zone diameters ranging from 8 to 14 mm. Compounds **3a-g** had modest antibacterial activity against *K. pneumonia*, with an inhibitory zone diameter of 10–15 mm. It is obvious that compound **3g**, which includes the OCH_3 group within its structure, demonstrated biological activities in the

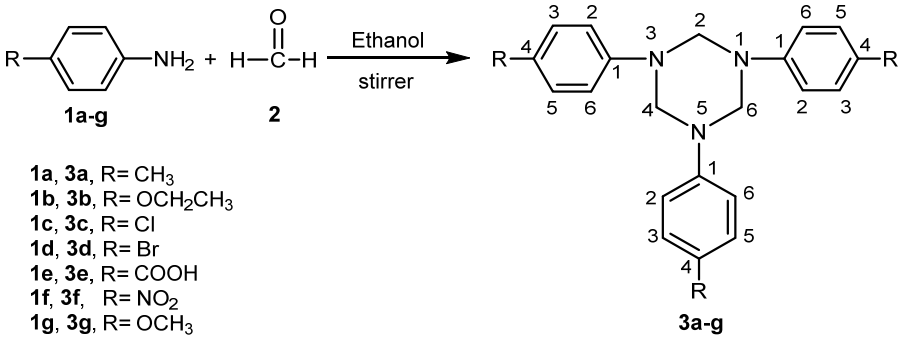

Scheme 1. Synthetic route to 1,3,5-hexahydrotriazines **3a**-**g**

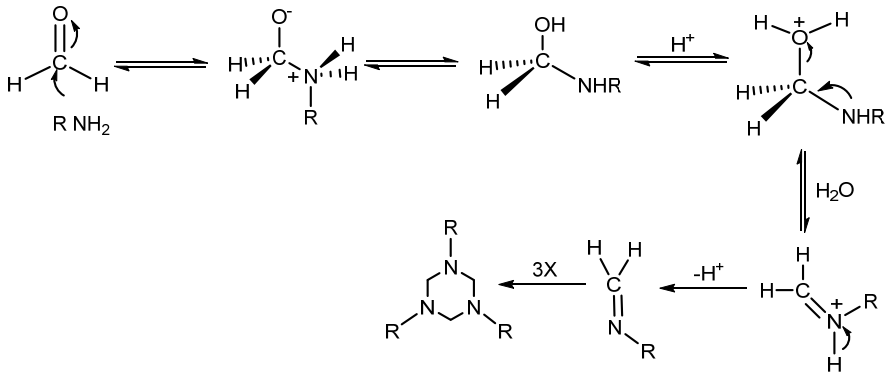

Fig 1. The mechanism of synthesis of hexahydrotriazines

studies used; however, variations in the other substituents have a significant effect on activity in several instances where screening chemicals demonstrated medium efficacy towards specific microbes (Table 1).

Inhibition of Biofilm Formation

The potential of *S. aureus* bacterial cells to create a biofilm was investigated, and the results are shown in Fig. 2. The bar chart shows the influence of compound **3g** at differing concentrations on the main *S. aureus* biofilm types. Despite these variations, it is crucial to remember that biofilm development decreases as concentration increases [29]. As shown in Table 2, Notably, at 40 and 100 µM, the inhibition of biofilm formation reached almost three-fifths as much as at 5 µM, which has been regarded as the optimal concentration to inhibit the growth of biofilm. After that decrease in inhibition of biofilm formation at 200 µM which nearly similarly inhibits the formation of biofilm as the concentration at 50 µM, Nevertheless, compound **3g** has a tendency to limit the biofilm population by approximately three-fold the amount that occurs in the absence of compound **3g**. The significant increases in the growth of biofilm during sub-inhibitory amounts of 10, 40, and 100 µM, which appears to be extremely important, is consistent as indication mounts that *S. aureus* reacts to sub-inhibitory concentrations of antibiotics via stimulating the growth of biofilm as well as altering the composition of the biofilm matrix [30-31]. The biofilm inhibition, which was observed as expected at concentrations 10, 40, and 100 µM, appears to follow a similar pattern to the decrease

Table 1. The compounds **3a**-**g** showed antimicrobial effects

Compounds	Inhibition zone diameter (mm)			
	S. aureus	*S. epidermidis*	*P. aeruginosa*	*K. pneumonia*
DMSO	-	-	-	-
3a	10	8	14	12
3b	12	9	14	13
3c	15	13	8	14
3d	11	15	12	10
3e	10	6	8	10
3f	8	9	13	15
3g	21	15	13	12
Ampicillin	27	20	29	30

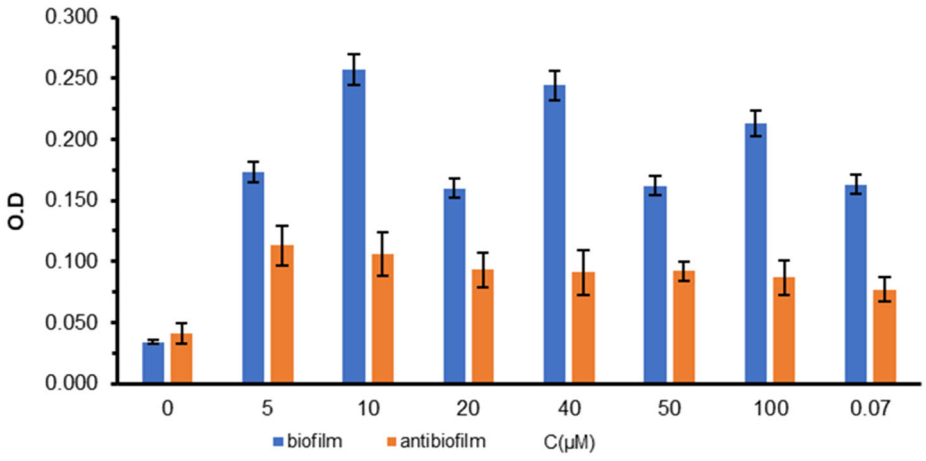

Fig 2. The activity of compound **3g** on *S. aureus* development and biofilm formation with a mixture of various amounts of the compound above. Two-way ANOVA analyses were used to study the differences between the biofilm and antibiofilm groups (p-value *< 0.05, **< 0.01, ***< 0.001)

Table 2. The inhibition percentage of compound **3g**

Concentrations of compound **3g**	Absorbance of biofilm	Absorbance of antibiofilm	Inhibition (%)
5	0.175	0.110	53.300
10	0.259	0.104	75.800
20	0.165	0.090	67.000
40	0.241	0.085	83.000
50	0.165	0.086	70.600
100	0.207	0.077	84.500
200	0.169	0.089	69.000
Control	0.053	-	-

in planktonic cell development, indicating that the last factor was strongly associated with both a decreased floating population as well as the anti-biofilm behavior [32]. The percentage inhibition for all concentrations was calculated using Eq. (1).

$$\%\ \text{inhib.} = \left(1 - \frac{\text{abs. of antibiofilm-abs. of control}}{\text{abs. of biofilm-abs. of control}}\right) \times 100 \qquad (1)$$

Docking Study

The molecular docking simulation study involving the powerful observed derivative **3g** within the attached site of GlcN-6-PS was explored by the use of AutoDock 4.2, which provides flexibility in docking from ligands inside the binding sites, either protein or enzyme. It possesses a tendency to utilize each of the rotated bonds of the ligands to produce a variety of configurations (10 by default), so the optimal modes were capable of being explored. The 3D structures of the enzyme as the interaction of all the produced conformists within an enzyme cavity are illustrated in Fig. 3. The estimated binding energy of the active compound **3g** was between −6.90 and −5.43 kcal mol^{-1}, while the inhibition constant (Ki) was 8.75 μM for the best-generated conformer as indicated by Table 3. The best-generated conformer (conformer 1) binds the active site with intermolecular energy equal to −8.69 kcal mol^{-1} and forms three hydrogen bonds with Thr 352, Ser 401 and Lys 603. As indicated by the X-ray crystallography, the

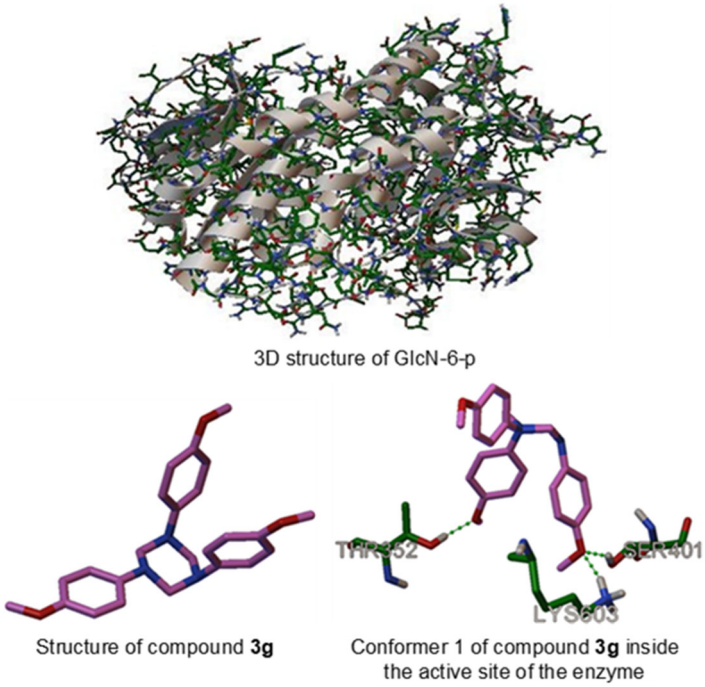

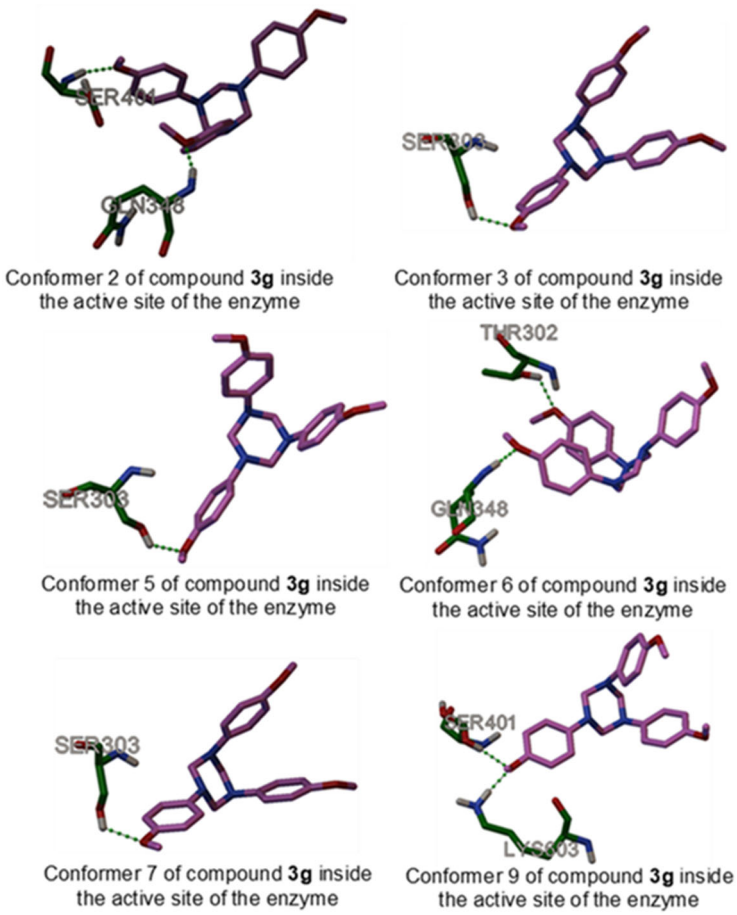

Fig 3. Docking of the potent derivative **3g** inside the binding pocket of (GlcN-6-p)

Table 3. Docking parameters of 3g inside the binding pocket of the enzyme

Conformers	Binding energy (kcal mol^{-1})	Inhibition constant (μM)	Intermolecular energy (kcal mol^{-1})	H-bonds	Bonding
1	−6.90	8.75	−8.69	3	Thr 352, Ser 401, Lys 603
2	−5.98	41.13	−7.77	2	Gln 348, Ser 401
3	−5.87	49.79	−7.66	1	Ser 303
4	−5.67	60.09	−7.55	0	-
5	−5.72	64.49	−7.51	1	Ser 303
6	−5.65	72.49	−7.44	2	Thr 302, Gln 348
7	−5.64	73.72	−7.43	1	Ser 303
8	−5.62	76.52	−7.41	0	-
9	−5.44	102.21	−7.23	2	Ser 401, Lys 603
0	−7.22	104.57	−5.43	0	-

binding pocket of the GlcN-6-PS includes the following residues: Cys 300, Gly 301, Thr 302, Ser 303, Ser 347, Gln 348, Ser 349, Thr 352, Val 399, Ser 401, Ala 602, and Lys 603 [20]. As illustrated from the docking results, the potent discovered hit binds the active site of the enzyme in a similar way to the substrate.

■ CONCLUSION

We created a number of hexahydro-1,3,5-triazine derivatives (**3a**-**g**) and verified the compounds via IR, ^{1}H-NMR, ^{13}C-NMR, and mass measurement. The synthetic substances have the potential to be effective antimicrobial and antibiofilm agents. The compound **3g** was found to inhibit biofilm formation at different concentrations of 5–200 μM. In contrast, a docking investigation was carried out to reveal the binding position of the ligand-enzyme complex for the potently identified hits.

■ ACKNOWLEDGMENTS

The authors would like to express their gratitude to the Chemistry Department of Mustansiriyah University College of Science for their cooperation in supplying the necessary materials for the successful completion of this research.

■ AUTHOR CONTRIBUTIONS

Nabel Bunyan Ayrim, Fadhel Rukhis Hafedh, and Ghosoun Lafta Mohsen conducted the synthesized material, and wrote the manuscript. Yasir Mohamed Kadhim, Abduljabbar Sabah Hussein, and Ahmed Mutanbi Abdula conducted calculations and analyses. Mohammed Mahdi Sami conducted bioassay experiments. Nabel Bunyan Ayrim, Ahmed Mutanbi Abdula, and Mohammed Mahdi Sami revised the manuscript. All authors agreed to the final version of the manuscript**.**

■ REFERENCES

[1] Venkatesan, N., Perumal, G., and Doble, M., 2015, Bacterial resistance in biofilm-associated bacteria, *Future Microbiol.*, 10 (11), 1743–1750.

[2] Nandakumar, V., Chittaranjan, S., Kurian, V.M., and Doble, M., 2013, Characteristics of bacterial biofilm associated with implant material in clinical practice, *Polym. J.*, 45 (2), 137–152.

[3] Puligundla, P., and Mok, C., 2017, Potential applications of nonthermal plasmas against biofilm-associated micro-organisms *in vitro*, *J. Appl. Microbiol.*, 122 (5), 1134–1148.

[4] Miquel, S., Lagrafeuille, R., Souweine, B., and Forestier, C., 2016, Anti-biofilm activity as a health issue, *Front. Microbiol.*, 7, 592.

[5] Cheng, B., Zhang, X., Zhai, S., He, Y., Tao, Q., Li, H., Wei, J., Sun, H., Wang, T., and Zhai, H., 2020, Synthesis of 1,2,3,4-tetrahydrobenzofuro[3,2-*d*]pyrimidines via [4+2] annulation reaction of 1,3,5-triazinanes and aurone-derived α,β-unsaturated imines, *Adv. Synth. Catal.*, 362 (18), 3836–3840.

[6] Chauhan, D.S., Quraishi, M.A., Wan Nik, W.B., and Srivastava, V., 2020, Triazines as a potential class of corrosion inhibitors: Present scenario, challenges and future perspectives, *J. Mol. Liq.*, 321, 114747.

[7] Singh, S., Manda, M.K., Masih, A., Saha, A., Ghosh, S.K., Bhat, H.R., and Singh, U.P., 2021, 1,3,5-Triazine: A versatile pharmacophore with diverse biological activities, *Arch. Pharm.*, 354 (6), 2000363.

[8] Bae, S.M., Kang, S.Y., and Song, J.H., 2021, Synthesis and cytotoxic activity of hexahydro-1,3,5-triazine derivatives through ring condensation, *Bull. Korean. Chem. Soc.*, 42 (6), 840–846.

[9] Qin, Y.G., Yang, Z.K., Fan, J., Jiang, X., Yang, X.L., and Chen, J.L., 2020, Synthesis, crystal structure and bioactivities of *N*-(5-(4-chlorobenzyl)-1,3,5-triazinan-2-ylidene)nitramide, *Crystals*, 10 (4), 245.

[10] Elmorsy, M.R., Abdel-Latif, E., Gaffer, H.E., Mahmoud, S.E., and Fadda, A.A., 2023, Anticancer evaluation and molecular docking of new pyridopyrazolo-triazine and pyridopyrazolo-triazole derivatives, *Sci. Rep.*, 13 (1), 2782.

[11] Mena, L., Billamboz, M., Charlet, R., Desprès, B., Sendid, B., Ghinet, A., and Jawhara, S., 2022, Two new compounds containing pyridinone or triazine heterocycles have antifungal properties against *Candida albicans*, *Antibiotics*, 11 (1), 72.

[12] Al-Sabagh, A.M., Kandile, N.G., Nasser, N.M., Mishrif, M.R., and El-Tabey, A.E., 2013, Novel surfactants incorporated with 1,3,5-triethanolhexahydro-1,3,5-triazine moiety as corrosion inhibitors for carbon steel in hydrochloric acid: Electrochemical and quantum chemical investigations, *Egypt. J. Pet.*, 22 (3), 351–365.

[13] Liu, H., Long, S., Rakesh, K.P., and Zha, G.F., 2020, Structure-activity relationships (SAR) of triazine

derivatives: Promising antimicrobial agents, *Eur. J. Med. Chem.*, 185, 111804.

[14] Dandia, A., Saini, P., Kumar, K., Sethi, M., Rathore, K.S., Meena, M.L., and Parewa, V., 2021, Synergetic effect of functionalized graphitic carbon nitride catalyst and ultrasound in aqueous medium: An efficient and sustainable synthesis of 1,3,5-trisubstituted hexahydro-1,3,5-triazines, *Curr. Res. Green Sustainable Chem.*, 4, 100170.

[15] Sujayev, A., Taslimi, P., Kaya, R., Safarov, B., Aliyeva, L., Farzaliyev, V., and Gulcin, I., 2019, Synthesis, characterization and biological evaluation of *N*-substituted triazinane-2-thiones and theoretical–experimental mechanism of condensation reaction, *Appl. Organomet. Chem.*, 34 (2), e5329.

[16] Pham, T.X., Pham, M.T., Cao, H.T., Nguyen, B.N., Nguyen, Q.H., and Trang, B.T., 2021, Study on the synthesis of 1,3,5-triazinane derivatives on copper-ferrite nanoparticles catalyst, *IOP Conf. Ser.: Earth Environ. Sci.*, 947 (1), 012028.

[17] Shah, D.R., Modh, R.P., and Chikhalia, K.H., 2014, Privileged *s*-triazines: Structure and pharmacological applications, *Future Med. Chem*., 6 (4), 463–477.

[18] Chmara, H., Andruszkiewicz, R., and Borowski, E., 1984, Inactivation of glucosamine-6-phosphate synthetase from *Salmonella typhimurium* LT 2 SL 1027 by N^{β}-fumarylcarboxyamido-L-2,3-diaminopropionic acid, *Biochem. Biophys. Res. Commun.*, 120 (3), 865–872.

[19] Borowski, E., 2000, Novel approaches in the rational design of antifungal agents of low toxicity, *Farmaco*, 55 (3), 206–208.

[20] Bearne, S.L., and Blouin, C., 2000, Inhibition of *Escherichia coli* glucosamine-6-phosphate synthase by reactive intermediate analogues: The role of the 2-amino function in catalysis, *J. Biol. Chem*., 275 (1), 135–140.

[21] You, S., Ma, S., Dai, J., Jia, Z., Liu, X., and Zhu, J., 2017, Hexahydro-*s*-triazine: A trial for acid-degradable epoxy resins with high performance, *ACS Sustainable Chem. Eng.*, 5 (6), 4683–4689.

[22] Kayarmar, R., Nagaraja, G.K., Naik, P., Manjunatha, H., Revanasiddappa, B.C., and Arulmoli, T., 2014, Synthesis and characterization of novel imidazoquinoline based 2-azetidinones as potent antimicrobial and anticancer agents, *J. Saudi Chem. Soc.*, 21, S434–S444.

[23] Ayrim, N.B., Balakit, A.A., and Lafta, S.J., 2022, Synthesis, characterization, molecular docking and biological activity studies of hydrazones with 3,4,5-trimethoxyphenyl moiety, *Egypt. J. Chem.*, 65 (6), 159–169.

[24] Rambabu, N., Ram, B., Dubey, P.K., Vasudha, B., and Balram, B., 2017, Synthesis and biological activity of novel (*E*)-*N*'-(substituted)-3,4,5-trimethoxybenzohydrazide analogs, *Orient. J. Chem*., 33 (1), 226–234.

[25] Matiadis, D., Karagiaouri, M., Mavroidi, B., Nowak, K., Katsipis, G., Pelecanou, M., Pantazaki, A., and Sagnou, M., 2020, Synthesis and antimicrobial evaluation of a pyrazoline-pyridine silver(I) complex: DNA-interaction and anti-biofilm activity, *BioMetals*, 34 (1), 67–85.

[26] Tomi, I.H.R., Al-Daraji, A.H.R., Abdula, A.M., and Al-Marjani, M.F., 2016, Synthesis, antimicrobial, and docking study of three novel 2,4,5-triarylimidazole derivatives, *J. Saudi Chem. Soc*., 20, S509–S516.

[27] Ismail, A.H., Abdula, A.M., Tomi, I.H.R., Al-Daraji, A.H.R., and Baqi, Y., 2021, Synthesis, antimicrobial, evaluation and docking study of novel 3,5-disubstituted-2-isoxazoline and 1,3,5-trisubstituted-2-pyrazoline derivatives, *Med. Chem*., 17 (5), 462–473.

[28] Ferhati, A., Malki, S., Bouchemma, A., Lefrada, L., Mazzouz, W., and Bouhenguel, M., 2019, Synthesis, characterization and antimicrobial activity of a new 1,3-bis(4-fluorophenyl)-5-butyl-1,3,5-triazacyclohexane, *J. New Technol. Mater.*, 9 (2), 17–21.

[29] Gondru, R., Kanugala, S., Raj, S., Ganesh Kumar, C., Pasupuleti, M., Banothu, J., and Bavantula, R., 2021, 1,2,3-Triazole-thiazole hybrids: Synthesis, *in vitro* antimicrobial activity and antibiofilm studies, *Bioorg. Med. Chem. Lett.*, 33, 127746.

[30] Schilcher, K., Andreoni, F., Dengler Haunreiter, V., Seidl, K., Hasse, B., and Zinkernagel, A.S., 2016,

Modulation of *Staphylococcus aureus* biofilm matrix by subinhibitory concentrations of clindamycin, *Antimicrob. Agents Chemother.*, 60 (10), 5957–5967.

[31] Shang, W., Rao, Y., Zheng, Y., Yang, Y., Hu, Q., Hu, Z., Yuan, J., Peng, H., Xiong, K., Tan, L., Li, S., Zhu, J., Li, M., Hu, X., Mao, X., and Rao, X., 2019, *β*-Lactam antibiotics enhance the pathogenicity of methicillin-resistant *Staphylococcus aureus* via SarA-controlled lipoprotein-like cluster expression, *MBio*, 10 (3), 00880–19.

[32] More, P.G., Karale, N.N., Lawand, A.S., Narang, N., and Patil, R.H., 2013, Synthesis and anti-biofilm activity of thiazole Schiff bases, *Med. Chem. Res.*, 23 (2), 790–799.